Critical properties of the ground-state localization-delocalization transition in the many-particle Aubry-André model

Taylor Cookmeyer,* Johannes Motruk, and Joel E. Moore
Department of Physics, University of California, Berkeley, California 94720, USA
and Materials Sciences Division, Lawrence Berkeley National Laboratory, Berkeley, California 94720, USA

(Received 22 January 2020; revised manuscript received 21 April 2020; accepted 21 April 2020; published 13 May 2020)

As opposed to random disorder, which localizes single-particle wave functions in one dimension (1D) at arbitrarily small disorder strengths, there is a localization-delocalization transition for quasiperiodic disorder in the 1D Aubry-André model at a finite disorder strength. On the single-particle level, many properties of the ground state at criticality have been revealed by applying a real-space renormalization-group scheme; the critical properties are determined solely by the continued-fraction expansion of the incommensurate frequency of the disorder. Here, we investigate the many-particle localization-delocalization transition in the Aubry-André model with and without interactions. In contrast to the single-particle case, we find that the critical exponents depend on a Diophantine equation relating the incommensurate frequency of the disorder and the filling fraction which generalizes the dependence, in the single-particle spectrum, on the continued-fraction expansion of the incommensurate frequency. This equation can be viewed as a generalization of the resonance condition in the commensurate case. When interactions are included, numerical evidence suggests that interactions may be irrelevant at at least some of these critical points, meaning that the critical exponent relations obtained from the Diophantine equation may actually survive in the interacting case.

DOI: 10.1103/PhysRevB.101.174203

I. INTRODUCTION

The localization of a system around random disorder is a problem originally addressed by Anderson [1]. More recently, once interactions were added, such systems were shown to exhibit many-body localization (MBL) [2–4] whereby local integrals of motion prevent thermalization. Random disorder makes such systems difficult to study theoretically (due to the necessity of disorder averaging) and experimentally (due to the challenge of engineering random disorder) [5].

Between random disorder and no disorder, there is quasiperiodic disorder as demonstrated by the Aubry-André-(Harper) (AA) model [6,7]

$$H_{\mathrm{AA}} = \sum_j h_j \hat{n}_j - J(\hat{c}_j^\dagger \hat{c}_{j+1} + \hat{c}_{j+1}^\dagger \hat{c}_j), \tag{1}$$

where $\hat{n}_j = \hat{c}_j^\dagger \hat{c}_j$, $\hat{c}_j^\dagger$ is a fermion creation operator on site j, and $h_j = \lambda J \cos(2\pi j\beta + \phi)$ for β an irrational number. The model can also be understood as the result of a tight-binding square-lattice Hamiltonian in the presence of a magnetic field yielding the famous Hofstadter butterfly when the hopping amplitudes are the same [8]. Within the single-particle spectrum, this model exhibits a one-dimensional (1D) localization-delocalization transition at $\lambda = 2$, which can be seen by considering the duality transformation $\hat{c}_k = \sum_j \exp(2\pi i\beta k j)\hat{c}_j/\sqrt{N}$ sending $\lambda \to 4/\lambda$ [6].[1]

Adding the simplest interaction term $H_{\mathrm{iAA}} = H_{\mathrm{AA}} + \sum_j V\hat{n}_j\hat{n}_{j+1}$ leads to the interacting Aubry-André (iAA) model. The localization of the ground state was theoretically predicted to persist once interactions were included [11,12]. Moreover, it was numerically demonstrated that the interacting model would exhibit many-body localization [13–18], and the universal properties of the MBL transition were predicted to be different between the random and quasiperiodic case [14], which has been shown in a toy model of MBL [19]. Interestingly, the MBL transition in the presence of interactions does not seem to exist close to $\lambda = 2$ at $V \ll J$ [20], but dynamical studies suggest that the MBL transition occurs at a large enough value of λ and $V \sim J$ [21,22].

One of the great advantages of this model, as opposed to random disorder, is that it can be more easily realized experimentally in cold-atom systems with interactions [23–26] and without interactions [27] or in photonic lattices without interactions [28]. Experiments on the interacting model have so far mostly focused on studying the MBL transition [23] and other aspects of MBL physics [24–26].

In addition to the fascinating higher-temperature properties of this system, the ground-state properties of this model, even in the free case, are still being explored. Recent work on

*tcookmeyer@berkeley.edu

[1]Note that when β is a Liouville number, the transition does not occur [9,10], which should therefore be excluded when we say "all β."

the noninteracting model has focused mainly on dynamical studies [29–33] or the critical properties of the transition [34,35], and numerous generalizations of the model have been introduced to generate a system with a mobility edge [36,37] or more topological features [38,39].

In this paper, we will focus on the ground-state critical properties of the (interacting) Aubry-André model where it was determined that the critical exponent of the correlation length $\nu = 1$ for the $\lambda = 2$ transition for all irrational β [6]. It has been known that the universality class of the single-particle ground state depended solely on the continued-fraction expansion of β [40]; only recently, however, with an explicit real-space renormalization-group (RSRG) scheme [41–43], the authors of Ref. [34] derived an expression for the dynamic critical exponent $z(\beta)$ for $\beta \ll 1$. Furthermore, as studied in Ref. [44], a similar transition occurs in the limit $\beta = 1/q$ with $q \to \infty$ at half-filling. (The authors of Ref. [44] claim that $\nu \approx 0.7$ instead of the usual $\nu = 1$, but we find that $\nu \approx 1$ later.)

The above RSRG scheme only works for the single-particle spectrum, and, although an RSRG for the middle of the spectrum exists [45], its assumptions are less physically clear, and the RSRG procedure depends strongly on β and only works at certain fillings. There exists therefore an open question about z's dependence on β and ρ where $\rho = N_F/N$ is the filling fraction. The value of z at different filling fractions determines how different parts of the energy spectrum scale with system size [46–48] and is therefore useful for understanding the multifractal properties of this system [49] as well as the multiparticle ground-state transition properties. Furthermore, it determines the low-temperature specific heat [49], and, as studied by Ref. [50], the Kibble-Zurek mechanism can be used to measure z at fixed system size. It was previously known that z does depend on the filling fraction [40,45], and it was incorrectly claimed that universality at half-filling was solely determined by the continued-fraction expansion in Ref. [40] (likely because the study was limited to only certain β), but we are aware of no classification of the universality relation between different filling fractions and different β.

In this work, we will present such a classification scheme. In a sense that we will make precise in Sec. III B the universality is controlled by the integers n and m that most nearly satisfy $n\beta - m = \rho$ where n and m are less than the system size. In the case when n and m are constant as a function of system size and the equation is exactly solved, the filling is called commensurate, n specifies the order of perturbation theory where there is a resonance between the Fermi momentum and the $\lambda \cos(2\pi\beta)$ term, and the transition occurs at $\lambda_c = 0$ with $\nu = n$ and $z = 1$. When n and m grow with system size, the filling is called incommensurate, and this equation is really a Diophantine equation that must be solved. The transition occurs at $\lambda_c = 2$, with $\nu = 1$, and z is specified by the sequence of values of n/N as $N \to \infty$.

Therefore, as we will show, the Diophantine equation that originates from $n\beta - m = \rho$ determines the universality class and reveals that, even at different fillings and different β, the universal properties of the transition can be the same. The same Diophantine equation has been considered for this model in other contexts such as the integer-quantum Hall effect as it is related to the Chern number of the band [51–54].

Once interactions are turned on, the ground-state phase diagram becomes richer [15] (see Ref. [55] for the bosonic version), but the critical exponent ν of the localization-delocalization transition does not seem sensitive to the interaction strength at half-filling [56]. Having the same value for all $\nu = 1$, it is an open question whether the dynamic critical exponent z remains the same, which would suggest that the universality class is insensitive to the interaction strength. In the integer quantum Hall effect, the value of ν appears to be the same as the noninteracting model, but the value of $z = 1$ seen in experiment is different than the $z = 2$ predicted by the noninteracting model (see, for instance, Ref. [57] and references therein).

We find that the interaction does not change the exponent z, which suggests that the Diophantine equation controls the universality even in the presence of interactions. As the Aubry-André model can be derived from a two-dimensional (2D) tight-binding Hamiltonian on a square lattice in the presence of a magnetic field, the robustness to interactions (and perhaps other perturbations) of the exponents may originate from the observation that the Diophantine equation can be derived nonperturbatively just considering the properties of the magnetic translation group where $n = \sigma_H$ is the total Hall conductivity [53,58]. In fact, in the incommensurate case, the Diophantine equation relates systems with the same Hall conductance per length σ_H/N.

The remainder of the work is organized as follows: Section II is devoted to some essential technical information needed to understand the rest of the paper. Section III focuses on the noninteracting AA model's critical properties. Sections III B and III C offer an explanation of the observed universal classes in terms of the Diophantine equation. We then move on to study the interacting model in Sec. IV, and we conclude in Sec. V.

II. PRELIMINARIES

Throughout all of this work, we will be considering periodic or antiperiodic boundary conditions and system sizes determined by the continued-fraction expansion for β, as is typical [9,34,49]. The continued-fraction expansion for β can be written as

$$\beta = n_0 + \cfrac{1}{n_1 + \cfrac{1}{n_2 + \cfrac{1}{n_3 + \cdots}}} = [n_0, n_1, n_2, \ldots], \tag{2}$$

where, without loss of generality, we set $n_0 = 0$ as it does not affect H_{AA}. Truncating the series at n_k gives a rational approximation to β as $\beta \approx M_k/N_k$ for M_k and N_k coprime. The $N \to \infty$ limit is taken by considering only the system sizes N_k in order to be able to satisfy (anti)periodic boundary conditions.

We will say two β's have the same asymptotic continued-fraction expansion if there exists some natural number k such that, for all $i > k$, the n_i appearing in the continued-fraction expansion are the same.

A quantum critical point occurs when the state of the system changes abruptly as some parameters in the Hamiltonian are tuned. In our case, the ground-state changes from being localized to delocalized as we move across the transition.

In a continuous quantum phase transition tuned by a single parameter λ and occurring at λ_c, the correlation length close to the transition scales as

$$\xi \sim \frac{1}{|\lambda - \lambda_c|^{\nu}}. \tag{3}$$

For localized single-particle wave functions, ξ can be identified with localization length of the wave function. That is, if the wave function is centered at i, the wave function decays as $e^{-|j-i|/\xi}$ for large $|j-i|$.

The consequences of the diverging critical length are called the critical properties; these properties include the correlation length exponent ν and the dynamic critical exponent z, which relates the scaling of a characteristic timescale $t \sim \xi^z$ or energy scale $E \sim \xi^{-z}$ to the correlation length.

The critical properties can be understood via the renormalization-group (RG) picture (see, for instance, Ref. [59]). Given a Hamiltonian $H(\vec{\lambda})$ with a set of parameters expressed as a vector $\vec{\lambda}$, the RG transformation traces over high-energy (or equivalently short-wavelength) degrees of freedom leading to a new Hamiltonian $H(\vec{\lambda}')$. Critical points are fixed points where $\vec{\lambda}' = \vec{\lambda} = \vec{\lambda}_c$, and near the fixed point, linearity of the RG transformation require that physical quantities take on a scaling form. For example, the energy per site has to behave as

$$E(\vec{\lambda} - \vec{\lambda}_c) - E(\vec{\lambda}_c) \sim b^{-(d+z)} \mathcal{F}(u_1 b^{y_1}, u_2 b^{y_2}, \ldots) \tag{4}$$

with $b > 1$ being a scaling factor typically identified with the correlation length ξ or the system size N, d is the dimensionality of the system, $\mathcal{F}$ is called a scaling function, the y_i are the eigenvalues of the RG transformation, and $\vec{u} = (u_1, u_2, \ldots)^T$ are the parameters $\vec{\lambda} - \vec{\lambda}_c$ transformed to be along eigenvectors of the RG transformation. If the exponent $y_i > 0$, u_i is said to be a relevant direction as $u_i b^{y_i}$ will grow as $\vec{\lambda} \to \vec{\lambda}_c$. Similarly, if $y_i < 0$, u_i is said to be an irrelevant direction. If $y_i = 0$, u_i is said to be a marginal direction.

The form of the scaling functions is only valid near the transition, and the data are said to collapse onto the scaling functions if, for many different parameter values, the scaling functions are the same. If one of the parameters is N, the system size, these are known as finite-size scaling functions and the exponents are determined by finite-size scaling. Deviations from collapsing to a single curve are known as finite-size effects if they disappear as $N \to \infty$. Two critical points are said to belong to the same universality class if all the exponents are the same, and if all the scaling functions are the same, up to a constant prefactor. (For a longer introduction of critical properties, see, for example, Refs. [59,60].)

We will determine the exponents by computing the following quantities: the (generalized) fidelity susceptibility and the superfluid fraction. The fidelity susceptibility is a powerful tool for studying quantum phase transitions (see Ref. [61] and references therein). With a generalized version, the exponents z, ν were extracted for the single-particle AA model [35], and a transition with $\beta \to 0$ in a controlled way with $\nu \approx 0.7$ was found at half-filling [44] (see also Fig. 6). The fidelity susceptibility is defined as

$$\chi_F = \lim_{\delta\lambda \to 0} \frac{-2 \ln F}{\delta\lambda^2}; \quad F = |\langle \Psi_0(\lambda + \delta\lambda) | \Psi_0(\lambda) \rangle|, \tag{5}$$

where $|\Psi_0(\lambda)\rangle$ is the ground state of H_{AA} with parameter value λ.

The superfluid fraction was used by Refs. [34,62,63] on this model. It is given by

$$\Gamma = N^2 \frac{d^2 E}{d\theta^2}, \tag{6}$$

where $E(\theta)$ is the ground-state energy with twisted periodic boundary conditions and is related to the curvature of the lowest band in the single-particle spectrum case [34].

These two quantities access certain critical exponents in the following way [34,61,64]:

$$\begin{aligned} \chi_F(\lambda = \lambda_{\max}) &\sim N^{\mu}; \\ \frac{\chi_F(\lambda = \lambda_{\max}) - \chi_F(\lambda)}{\chi_F(\lambda)} &= f(N^{1/\nu}(\lambda - \lambda_{\max})); \\ \Gamma &= N^{2-z} g(N^{1/\nu}(\lambda - \lambda_c)). \end{aligned} \tag{7}$$

Here, $\lambda_{\max}$ is the value of λ that maximizes χ_F and is typically close to λ_c, and μ, the critical adiabatic dimension, is defined via the first equation [61].[2] The functions $f(x)$ and $g(x)$ are scaling functions. The exponent ν has been extracted in the interacting Aubry-André model before using a different quantity in Ref. [56].

Through Γ, z is difficult to determine as it does not have a peak, but we can extract the value of z in the $V = 0$ case through the generalized fidelity susceptibility via the following equation [35,66]:

$$\chi_{F,2+2r} = \sum_{n \neq 0} \frac{|\langle \Psi_n(\lambda) | H_I | \Psi_0(\lambda) \rangle|^2}{(E_n - E_0)^{2+2r}}, \tag{8}$$

where $H = H_0 + \lambda H_I$, and the sum is over all excited states $|\Psi_n(\lambda)\rangle$. When $r = 0$, we recover the usual fidelity susceptibility. It is known that $\chi_{F,2+2r} \sim N^{\mu+2zr}$ at the critical point [35,66], which provides an efficient means of extracting μ and z. In the free case, for arbitrary fillings, this is a possible computation because only $\sim N^2$ states contribute (see Appendix A); once we compute z from the generalized fidelity susceptibility, that same value is used to collapse the Γ curves onto each other.

A. Boundary conditions

Since we are interested in the thermodynamic limit, we expect that boundary conditions do not play such an important role. However, we find that the boundary conditions do influence the finite-size scaling collapse. Therefore, we want to make as consistent a choice as possible. The easiest way to continue is not to consider the fermionic Hamiltonian form

[2]Note that there is misrepresentation of the fidelity susceptibility in the literature that says $\chi_F \sim N^{2/\nu}$, but this is not correct. This can most easily be seen in the Kitaev honeycomb model where $\mu \approx \frac{5}{2}$ and $\nu \approx 1$ [65]. However, it is quite common that $\mu = 2/\nu$, and we will always be able to compute ν via the universal functions. We find that $\mu \approx 2/\nu$ for this model with the largest deviation occurring for $\beta =$ "0" (see Fig. 6).

TABLE I. Choice of phase ϕ and P_F for a given N and N_F when computing Γ and $\chi_{F,2+2r}$.

	N_F even	N_F odd
N odd	$\phi = \pi, P_F = 1$	$\phi = 0, P_F = -1$
N even	$\phi = \pi/2, P_F = 1$	$\phi = 3\pi/2, P_F = -1$

(1) above but to consider the spin-$\frac{1}{2}$ Hamiltonian

$$H = -\sum_{j=1}^{N-1} J(S_j^+ S_{j+1}^- + \text{H.c.}) - AJ(S_N^+ S_1^- e^{i\theta} + \text{H.c.}) + \sum_{j=1}^{N} V S_j^z S_{j+1}^z + h_j S_j^z, \tag{9}$$

where $A = 1$ corresponds to periodic boundary conditions (PBC) and $A = -1$ corresponds to antiperiodic boundary conditions (ABC). We have made the twist in the boundary condition θ explicit. When we map back to the fermionic Hamiltonian via a Jordan-Wigner transformation, we find that, up to a shift in the chemical potential,

$$H = -\sum_{j=1}^{N-1} J(\hat{c}_j^\dagger \hat{c}_{j+1} + \text{H.c.}) - P_F AJ(\hat{c}_N^\dagger \hat{c}_1 e^{i\theta} + \text{H.c.}) + \sum_j h_j \hat{n}_j + V \hat{n}_j \hat{n}_{j+1}, \tag{10}$$

where the number of fermions N_F determines $P_F = (-1)^{N_F} = (-1)^N \prod_i (2S_i^z)$. We will set $J = 1$ from here on in. This is a number-conserving Hamiltonian, so we have the good quantum number $N_F = N_\uparrow$, the number of spin ups, and we will study it at the filling $\rho = N_F/N = N_\uparrow/N$.

Within the spin language, the Hamiltonian exhibits spin-flip symmetry, which relates the ground states $\Psi(\lambda/|J|, \text{sgn}(J), A, \phi, N_\uparrow) \leftrightarrow \Psi(\lambda/|J|, \text{sgn}(J), A, \phi + \pi, N - N_\uparrow)$. Since $\text{sgn}(\Gamma) = (-1)^{N_F}$, the data cannot be collapsed well if N_F takes both even and odd values. We fix this by using the setup in Table I. Essentially, this guarantees keeping the spin Hamiltonian the same, though using $\phi \in \{0, \pi\}$, being not a generic value of ϕ, means that the collapse fails in certain cases and other angles need to be tried.

The specification in Table I means we are looking at a system with ABC in the single-particle spectrum which is equivalent to studying the $J > 0$ model with PBC when N is odd (because of the transformation $\hat{c}_j \to -\hat{c}_j$ for even j).

III. NONINTERACTING CASE $V = 0$

We now study how Γ and $\chi_{F,2+2r}$ behave in the free case. We consider only β with a periodic continued-fraction expansion, and, for simplicity, only those which are asymptotically $[\ldots, n, n, n, n, \ldots]$. Specifically, we will focus on the following incommensurate ratios:

$$\beta_{nm} = [0, m, n, n, n, \ldots] = \frac{1}{m + \beta_{nn}}, \tag{11}$$

where $\beta_{nn} = (\sqrt{n^2+4} - n)/2$ are the metallic means. We will also consider $\beta =$ "0" with best rational approximation $1/N$ for all N [44].

A. Numerical results

We are able to use this to reproduce the results [34,40] (see also Ref. [35]) for the critical exponents z and ν in the single-particle spectrum. In this case, z only depends on the asymptotic continued fraction expansion. For $\beta \ll 1$, the exponent z is in fact given by [34]

$$z(\beta_{nm}) \approx 1.1662 \frac{\beta_{nn}^{-1}}{\log\left(\beta_{nn}^{-1}\right)}, \tag{12}$$

where it is clear that $z \to \infty$ as $\beta \to 0$. Additionally, as was shown by Aubry and André [6], the correlation length goes as

$$\xi^{-1} \sim \ln\left(\frac{\lambda}{2}\right), \quad \lambda \geqslant 2 \tag{13}$$

implying $\nu = 1$.

From now on, we consider fillings with an extensive number of particles. We focus on the sector with $N_F = \lfloor \rho N \rceil$ where $\lfloor x \rceil$ rounds x to the nearest integer, and $\rho \in (0, 1)$ is the filling fraction.

This investigation leads to a series of observations. First, at half-filling $\rho = \frac{1}{2}$, we notice that not all system sizes have the same scaling functions as seen in Fig. 1 for the golden ratio β_{11}, despite the exponents being the same to several decimal points. The rational approximations to $\beta_{11} \approx M_k/N_k$ from the continued-fraction expansion are given by F_k/F_{k+1} where $F_k = 1, 1, 2, 3, 5, \ldots$ are the Fibonacci numbers satisfying $F_1 = 1$, $F_2 = 1$, and $F_{k+1} = F_k + F_{k-1}$. In this case, the sequence of denominators N_k breaks into three subsequences $34, 144, 610, \ldots$; $21, 55, 233, 987, \ldots$; and $89, 377, 1597, \ldots$ each with a separate scaling function. This separation into three subsequences has been observed in the exact RSRG scheme [45] and in multifractality studies [49] and the value of the exponent for β_{11} agrees with that of Refs. [9,45,49] for the scaling of the middle part of the spectrum. As a more general pattern, when considering β_{1m} for any m, we also find that there are three scaling functions with the same exponent z at half-filling.

However, when we now consider the silver ratio, β_{22} and associated β_{2m} at $\rho = \frac{1}{2}$, we notice that β_{22} splits into only two subsequences with separate scaling functions and β_{21} splits into only one, and, between the two β, z is different (see Fig. 2). Moreover, when β_{22} is at a filling of $1 - 1/\sqrt{2}$, it has the same exponent as β_{21} at half-filling and the scaling functions are the same after a global rescaling suggesting that they belong to the same universality class. We have also checked explicitly that β_{22} and β_{21} are in the same universality class at $\rho = \frac{1}{3}$.

Since the second derivative of the energy $\partial^2 E/\partial\lambda^2 = \chi_{F,1}$, this quantity also has access to the exponent z, so we plot $\chi_{F,1}/N$ vs ρ at $\lambda = 2$ in Fig. 3. We notice that a fractal shape emerges, and the similarity of the fractal shape for β_{21} at $\rho = \frac{1}{2}$ and β_{22} at $\rho = 1 - 1/\sqrt{2}$ suggests that they belong to the same universality class.

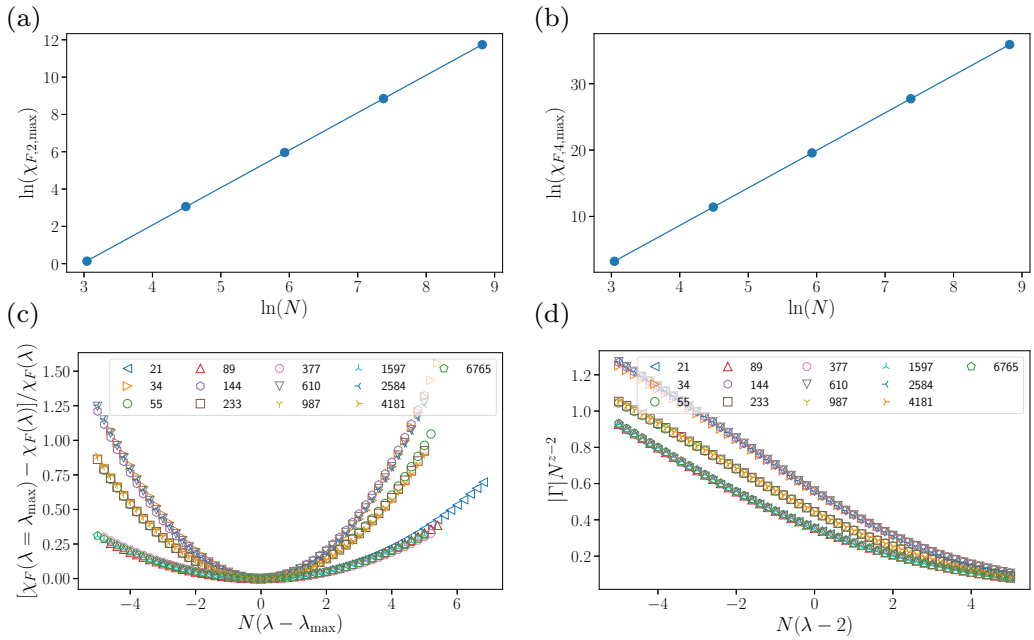

FIG. 1. Scaling of the generalized fidelity susceptibility $\chi_{F,2+2r}$ and the superfluid fraction Γ for $\beta=\beta_{11}=(\sqrt{5}-1)/2$ at filling $\rho=\frac{1}{2}$ with the angle and P_F specified by Table I. (a), (b) Show how the maxima of $\chi_{F,2+2r}\sim L^{\mu+2zr}$ from which $\mu=2.0$ and $z=1.8285$ are extracted. In (c) and (d), the scaling of χ_F and Γ, respectively, is consistent with $\mu=2/\nu=2.00$, and $z=1.8285$ collapses all the Γ curves onto three scaling functions.

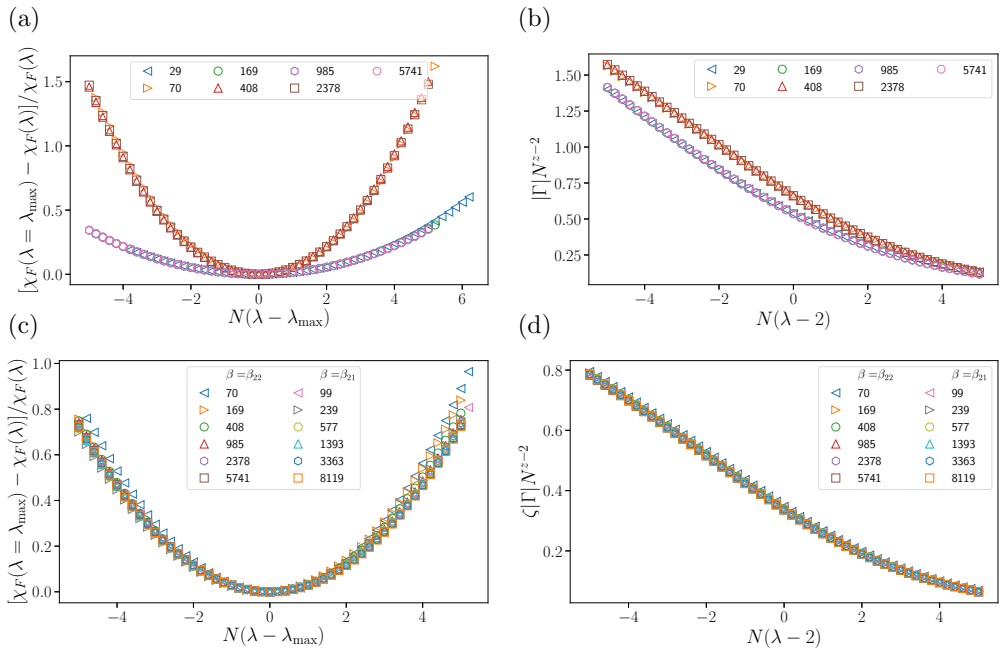

FIG. 2. In (a) and (b), the collapse of χ_F and Γ, respectively, onto the scaling functions is plotted for $\beta=\beta_{22}$, and there are two separate scaling functions: one for N even and one for N odd. Again, $\mu=2/\nu=2.00$, and the same value of $z=2.0875$ scales all Γ curves onto each other. In (c) and (d), the same quantities are plotted for $\beta=\beta_{21}$ with a filling of $\rho=\frac{1}{2}$ when $N=99, 239, 577, 1983, 3363, 8119$, and $\beta=\beta_{22}$ with a filling of $\rho=1-1/\sqrt{2}$ otherwise. Still $\nu=1$, but $z=1.575$. Up to the normalization of Γ ($\zeta=1.0$ for β_{21} and $\zeta=0.6605$ for β_{22}) the two scaling functions are the same, suggesting that the universality class of the $\lambda_c=2$ transition is the same for β_{21} at half-filling and β_{22} at $\rho=1-1/\sqrt{2}$. The finite-size effects are worse for β_{22} because of the irrational filling. However, once N is large enough for the filling to be well approximated, the collapse is very good. ϕ and P_F are set according to Table I

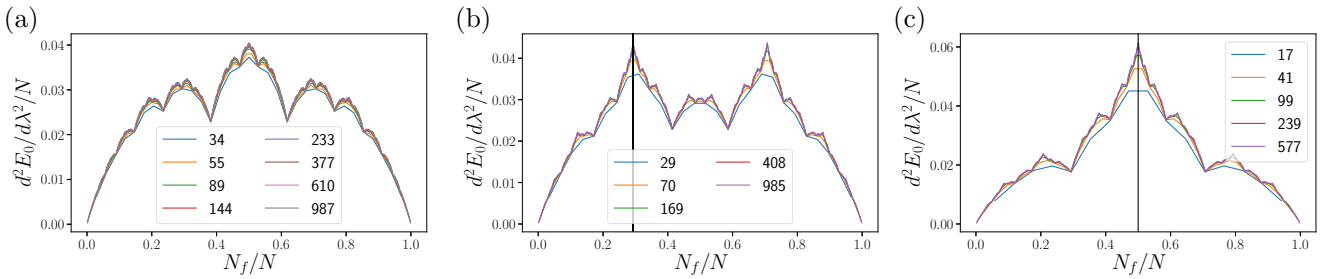

FIG. 3. The second derivative of the ground-state energy per particle at $\lambda = 2$, $d^2E/d\lambda^2/N$, for (a) β_{11}, (b) β_{22}, and (c) β_{21}, is plotted against N_F/N, the filling fraction. A clear fractal structure emerges. Note the difference between β_{22} and β_{21} at half-filling, and note the similarity at the filling fraction indicated by the black vertical line at $\rho = 1 - 1/\sqrt{2}$ for β_{22} and $\rho = \frac{1}{2}$ for β_{21} where the same critical exponents and scaling functions are observed (see Fig. 2).

When we broaden our scope to β_{3m} and β_{4m} (beyond which, the number of accessible system sizes is small) and to filling fractions $\frac{1}{3}$ and $\frac{1}{4}$, we find the exponents in Table II. Based on these results, we conjecture that when the filling is $1/q$ and the filling fraction is β_{pm}, the exponents can be different if the greatest common divisor of q and p is not 1. (See Sec. III C for more details and Appendix D.)

Motivated by Ref. [56], we also consider commensurate fillings $\rho = n\phi - m$ for $n = 1, 2, 3, 5$ and m chosen so that $\rho \in (0, 1)$. In this case, the transition occurs not at $\lambda = 2$, but at $\lambda = 0$. That is, a gap immediately opens up at nth order in perturbation theory because of the close relationship between the Fermi momentum $k_F = \pi\rho$ and the perturbation at $k = 2\pi\beta$. The results are shown in Fig. 4. For all n, we consider $\phi = \beta_{11}$ and find that $\nu = n$ and $z = 1$ as explained by the perturbation theory analysis in Ref. [44]. For $n = 2$, we additionally show $\beta = \beta_{12}$ and $\beta = \frac{1}{4}$ at the corresponding commensurate fillings and see that they collapse together onto the same curve.

B. Our Diophantine equation conjecture

We will argue that the critical properties observed in the previous section can be understood by a Diophantine equation. This equation determines the universality class both in commensurate and incommensurate fillings.

In the case that the filling is commensurate, there is a resonance at nth order in perturbation theory because $\rho = n\beta - m$ for integers n and m, and n determines the universality class of the transition as $\nu = n$ and $z = 1$ [44]. As noted above, the transition always occurs at $\lambda_c = 0$, and we numerically see that the scaling functions are all the same.

When the filling is not commensurate, we can still consider the same equation. Noting that we always approximate $\beta \approx \beta_k = M_k/N_k$ and $N_F = \lfloor \rho N_k \rceil$, $\rho = n\beta - m$ becomes

$$M_k Q_k - P_k N_k = \pm N_F, \tag{14}$$

where (Q_k, P_k) has replaced (n, m). Since N_k, M_k, and N_F are all integers, and we are still searching for integers Q_k and P_k, Eq. (14) has the form of a Diophantine equation. We emphasize that this Diophantine equation is

TABLE II. The exponents extracted from finite-size scaling at various fillings. The number of scaling functions p is determined by scaling collapse as in Figs. 1 and 2 and via the Diophantine equation where it is determined by the period of the repeating values of $|Q_k|/N_k$ for large k for β_{mn}. In the cases where z and p agree, the same sequence of $|Q_k|/N_k$ appears suggesting the Diophantine equation (14) probes the universal properties. Indeed, the Diophantine equation predicts which β and ρ to consider to fill the last column, and predicts why differences only occur in the first column when β_{mn} has m even. If no value of z is reported (indicated by a "-"), it is because a good collapse was not seen for system sizes $N < 10^4$; in those cases, p was determined via the Diophantine equation alone. It is worth noting that a value $z \approx 2$ is the expected value for a "generic" filling as that is near the peak of the distributions of $1/\alpha$'s in the multifractal analysis [34,49]. For β_{2n}, an error bar of ± 0.01 is given because the large value of p means only two curves fell into each universality class for $N < 10^4$; yet, the finite-size scaling is very sensitive to z due to the large system sizes, and the collapse does not work well beyond the reported range.

β	(z, p), $\rho = \frac{1}{2}$	(z, p), $\rho = \frac{1}{3}$	(z, p), $\rho = \frac{1}{4}$	Other (ρ, z, p)
$\beta_{11} = 1 - \beta_{12}, \beta_{14}, \beta_{13}$	(1.8285,3)	(2.00,4)	(2.0,6)	
β_{22}	(2.0875,2)	(1.97 ± 0.01,4)	(–,8)	$(1 - 1/\sqrt{2}$,1.575,1)
$\beta_{21} = 1 - \beta_{23}, \beta_{25}$	(1.575,1)	(1.97 ± 0.01,4)	(2.09,2)	
β_{24}	(2.0875,2)	(1.97 ± 0.01,4)	(–,8)	
β_{33}	(2.0,3)	(2.24,2)	(–,6)	$(1/(3\beta_{31})$,1.67,1)
β_{32}	(2.0,3)	(2.02,1)	(–,6)	$(\beta_{32}/(3\beta_{31})$,1.67,1)
β_{31}	(2.0,3)	(1.67,1)	(–,6)	
β_{44}	(2.374,2)	(–,4)	(–,2)	
β_{43}	(1.518,1)	(–,4)	(2.57,1)	
β_{41}	(1.518,1)	(–,4)	(1.815,1)	

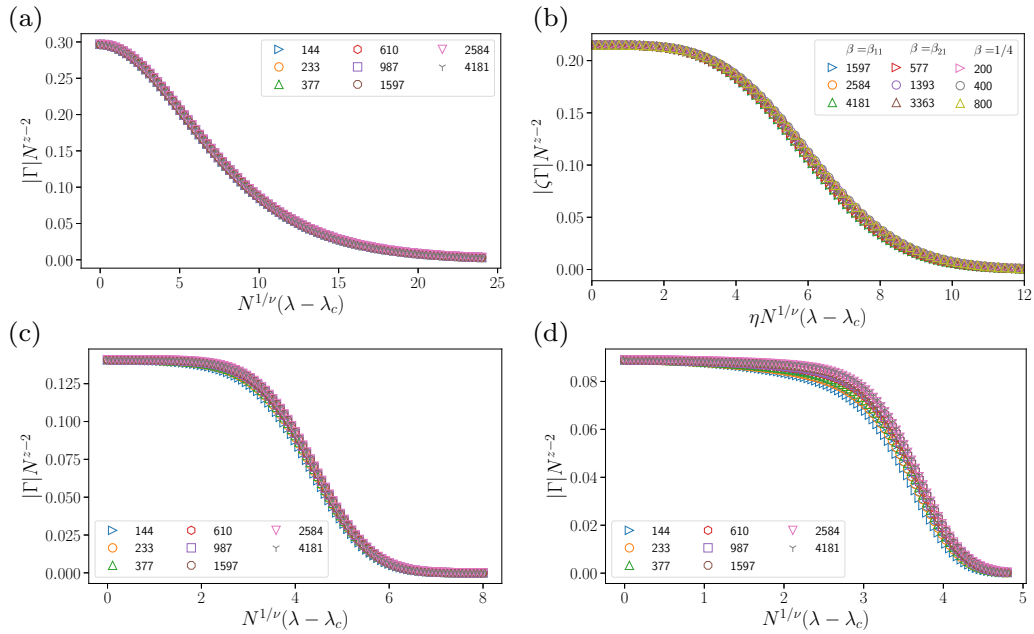

FIG. 4. At commensurate filling, the transition moves from $\lambda_c = 2$ to 0 because the resonance condition is fulfilled for some fixed $n = \nu$. The dynamic critical exponent is always $z = 1$. In (a) we have $\beta = \beta_{11}$ and $\rho = 1 - \beta_{11}$ with $\nu = 1$. In (b) we plot several N for $\beta = \{\beta_{11}, \beta_{21}, \frac{1}{4}\}$ at $\rho = \{2\beta_{11} - 1, 2\beta_{21} - 1, \frac{1}{2}\}$ and we see that they have the same $\nu = 2$ and $z = 1$. The curves collapse onto each other when $\zeta = \{1, 0.7007, 0.6755\}$ and $\eta = \{1, 1, 1.565\}$. In (c) we have $\beta = \beta_{11}$ and $\rho = 3\beta_{11} - 2$ with $\nu = 3$. In (d) we have $\beta = \beta_{11}$ and $\rho = 5\beta_{11} - 3$ with $\nu = 5$. Note that the finite-size effects get worse as $\rho \to 0$.

derived from seeking integers (Q_k, P_k) that nearly satisfy $Q_k\beta - P_k = \rho$.

This Diophantine equation has already been studied both in the limit of $\lambda \ll 1$ and $\lambda \gg 1$. For $\lambda \ll 1$, the most important terms in perturbation theory are those with large n that nearly satisfy $\rho = n\beta - m$ [67]. In the opposite limit, when $\lambda \gg 1$, if we consider when the dominant component of the single-particle wave function changes as we tune ϕ, we get the same Diophantine equation [51], where Q_k is the Chern number [52,53].

Because M_k and N_k share no divisor except 1, there are infinitely many solutions (Q_k, P_k) to Eq. (14). We restrict the solutions $|Q_k| \leqslant N_k/2$ (as the resonance condition is satisfied at the lowest value of Q_k) and, of the two possible values of the right-hand side of Eq. (14), we pick the one that gives the smallest $|Q_k|$. When solving the Diophantine equation for different N_k, N_F, we find that the value of $|Q_k|/N_k$ for large k has a period of p different values breaking the sequence of denominators into p subsequences. We see in Table II that p is also the number of scaling functions (e.g., $p = 3$ for β_{11} and $p = 2$ for β_{22} at half-filling) seen in every case we can check. When we compare the values of $|Q_k|/N_k$ with different β and different filling ρ, we find that the sequence is the same if and only if the exponent z, p, and the scaling functions are the same. We therefore conjecture that $|Q_k|/N_k$ for $k \gg 1$ determines the universality class, and p predicts the different versions of the scaling functions. This conjecture is our main result, and, in the next section, we will see that, with this conjecture, we can understand all the other above observations.

An explicit example

Before we continue, let us work through a concrete example to show how the Diophantine equation reveals information about the universality class. Consider the silver ratio $\beta_{22} = \sqrt{2} - 1$ and $\beta_{21} = 1/\sqrt{2}$. Both β's continued fraction expansions are the same after the first term and, in the single-particle spectrum, they would therefore be in the same universality class [34,40–43]. Let us now solve the Diophantine equation in the case of half-filling (i.e., $N_F = \lfloor N_k/2 \rfloor$ with $\lfloor\cdot\rfloor$ denoting the floor function) where a different result will emerge.

The silver ratio's continued-fraction expansion is related to the Pell numbers given by $P_k = 1, 2, 5, 12, 29, 70, \ldots$ where $P_1 = 1$, $P_2 = 2$, and $P_{k+1} = 2P_k + P_{k-1}$. The best rational approximations to β_{22} are given by $M_k = P_k$ and $N_k = P_{k+1}$, while the best rational approximations to β_{21} are given by $M_k = P_k$ and $N_k = P_k + P_{k-1}$. After specifying M_k, N_k, and $N_F = \lfloor N_k/2 \rfloor$, there are an infinite number of integer solutions (Q_k, P_k) to Eq. (14), but we find the solution with $|Q_k| \leqslant N_k/2$ for both $\pm N_F$, and, of those, we pick the solution with the smaller value of $|Q_k|$. With $\lceil\cdot\rceil$ denoting the ceiling function, We find that $|Q_k| = 1, 6, 6, 35, 35, \ldots = P_{2\lceil(k+1)/2\rceil}/2$ for β_{22} and $|Q_k| = 0, 1, 2, 5, 12, \ldots = M_{k-1}$ for β_{21}. Then, for β_{22} and large enough k, $|Q_k|/N_k = \ldots, q_1, q_2, q_1, q_2, \ldots$ where $q_1 = \frac{1}{2}$ and $q_2 = (\sqrt{2} - 1)/2 \approx M_k/(2N_k)$, whereas, for β_{21} and large enough k, $|Q_k|/N_k = \ldots, q_3, q_3, q_3, \ldots$ with $q_3 = 1 - 1/\sqrt{2}$.

We would then conjecture that β_{22} and β_{21} belong to two different universality classes at half-filling, which is demonstrated in Fig. 2. The periodicity of the values of $|Q_k|/N_k$

corresponds to the two scaling functions for β_{21} and the one scaling function for β_b.

If we consider instead the golden ratio $\beta_{11} = (\sqrt{5}-1)/2$ and other β's with the same asymptotic continued-fraction expansion, they will ultimately have the same repeating part of the sequence of $|Q_k|/N_k$ with a periodicity of three at half-filling. Our Diophantine equation conjecture would then predict that they are in the same universality class, as was seen by Ref. [40] and as we observe numerically (see Table II and Fig. 1).

C. Discussion

To connect our conjecture with the past results, we want to show that the single-particle sector's universal properties are solely determined by the continued-fraction expansion. It is well known that Diophantine equations can be solved exactly with knowledge of the continued-fraction expansion of $\beta = [0, n_1, n_2, \ldots]$. First, we solve the case where $\pm N_F = \pm 1$, which is given by $(Q'_k, P'_k) = \pm(N_{k-1}, M_{k-1})$ if $n_{k-1} \neq 1$ and $(Q'_k, P'_k) = \pm(N_{k-2}, M_{k-2})$ otherwise. Then, the solution to the original equation is given by $Q_k = Q'_k N_F \bmod N_k$ and $P_k = P'_k N_F \bmod M_k$.

Immediately, when $N_F = \pm 1$, we compute that $|Q_k|/N_k = N_{k-1}/N_k$ (or N_{k-2}/N_k). It suffices to show, then, that N_{k-1}/N_k just depends on the asymptotic part of the continued fraction expansion. This can easily be shown in the case of $\beta = \beta_{nm}$ since (denoting $\beta_k = M_{\beta,k}/N_{\beta,k}$)

$$\frac{M_{\beta_{nm},k}}{N_{\beta_{nm},k}} = \frac{N_{\beta_{nn},k}}{N_{\beta_{nn},k} m + M_{\beta_{nn},k}}. \tag{15}$$

Note that, as $M_{\beta_{nn},k}/N_{\beta_{nn},k}$ is a reduced fraction, $M_{\beta_{nm},k}/N_{\beta_{nm},k}$ is as well. Therefore,

$$\lim_{k\to\infty} N_{\beta_{nm},k}/N_{\beta_{nm},k-1} = N_{\beta_{nn},k}/N_{\beta_{nn},k-1} \approx n + \beta_{nn}, \tag{16}$$

where we used $M_{\beta_{nn},k}/N_{\beta_{nn},k} \to \beta_{nn}$ as $k \to \infty$. This argument can be easily extended to the general case, so $p = 1$ and $|Q_k|/N_k$—and therefore, under our conjecture, the universality class—is determined solely by the asymptotic continued-fraction expansion consistent with the RSRG scheme [34,41,42].

Outside of the single-particle spectrum, we worked an explicit example in Sec. III B that showed β_{21} and β_{22} are predicted not to be in the same universality class at half-filling. Additionally, we can explain why the fractal shape in Fig. 3 appears. In Appendix B, we use the Diophantine equation and our conjecture to derive that the universality class is the same at a density of ρ and a density of ρ/β_{nn} for β_{nn} and incommensurate fillings. This fact would reproduce a fractal shape as ρ, ρ/β_{nn}^k, and $\rho\beta_{nn}^k$ will all have the same z for any integer k.

Notably, this does not hold for nonmetallic means such as β_{21} where, for instance, $\rho = \frac{1}{2}$ and $\rho = 1/\sqrt{2} - \frac{1}{2}$ can be shown to be related with the Diophantine equation trivially, which is also seen as the second largest peak within the fractal structure in Fig. 3(c). We have explicitly checked that β_{21} at this filling not only has the same z but the scaling function controlling Γ is the same up to a numerical prefactor.

Furthermore, we can consider β_{nm} and, in a way that can be made rigorous as in the calculation of Appendix B, we can see

$$Q\beta_{nm} - P = \rho \iff (Q - Pm) - P\beta_{nn} = \frac{\rho}{\beta_{nm}}. \tag{17}$$

Using the above result, we see β_{nm} at a filling of ρ should have the same exponent as β_{nn} at a filling of $\rho' = \rho/\beta_{nm}$. This observation predicts the relationship between β_{21} and β_{22} at half-filling and $\rho = (1 - 1/\sqrt{2})$ filling, respectively, as particle-hole symmetry relates a filling of ρ and $1-\rho$ [see Figs. 2(c) and 2(d)].

Finally, consider the similar explicit calculation here for n odd:

$$\begin{aligned}
0 &= Q\frac{1}{m+\beta_{nn}} + P \pm \frac{1}{2} \iff \\
0 &= (Q + Pm) + P\beta_{nn} \pm \frac{1}{2}(m + \beta_{nn}) \\
&= \begin{cases} \left(Q + Pm \pm \frac{m-n}{2}\right) + P\beta_{nn} \pm \frac{1}{2\beta_{nn}} & \text{if } m \text{ is odd,} \\ \left(Q + Pm \pm \frac{m}{2}\right) + P\beta_{nn} \pm \frac{\beta_{nn}}{2} & \text{if } m \text{ is even} \end{cases} \\
&= \begin{cases} P' + Q'\beta_{nn} \pm \frac{1}{2\beta_{nn}} & \text{if } m \text{ is odd,} \\ P'' + Q'\beta_{nn} \pm \frac{\beta_{nn}}{2} & \text{if } m \text{ is even,} \end{cases}
\end{aligned} \tag{18}$$

where P', P'', and Q' are integers. In the two cases above, if n is odd, we have been able to absorb an integer into the definition of P' or P'' to get rid of the dependence on m. Since the critical properties of β_{nn} at $\beta_{nn}/2$ and $1/(2\beta_{nn})$ are the same as those at $\rho = \frac{1}{2}$, then all the β_{nm} have the same exponents at half-filling if n is odd.

This breaks down if n is even because the m odd case does not give an integer value of P'. Generically, we expect that if $\rho = 1/q$, $\beta = \beta_{nn}$ and n and q are coprime, then all of the β_{nm} will be in the same universality class at filling $\rho = 1/q$. However, if n and q share a common factor, there will be separate classes. If we consider a filling of $\frac{1}{3}$, this would allow for β_{3m} to split into three separate universality classes based on the residual of m mod 3. We indeed observe this numerically for the systems we can access.

To summarize, the Diophantine equation can predict the fractal structure of Fig. 3, explains the number of universal curves p, predicts which fillings and which β belong to the same universal classes, and, in commensurate filling, specifies the exponent ν directly.

IV. INTERACTING CASE $V \neq 0$

The Diophantine equation description of the universality seems particularly pathological, so we check whether it persists in the presence of the simplest form of interactions as that is the most interesting perturbation. Trivially, it will persist with a shift in the chemical potential, but p-wave pairing terms would destroy it because well-defined fermion number is necessary for the Diophantine equation. Another possible addition would be to consider farther neighbor hopping which, however, goes beyond the scope of this work.

In order to study the interacting model, we use the density-matrix renormalization group (DMRG) [68] on Eq. (9) with $V \neq 0$ as implemented by the iTensor library [69]. We must have PBC or ABC to compute Γ to extract z. This choice of boundary condition makes convergence in the matrix product state (MPS) bond dimension slower, as a truncation error

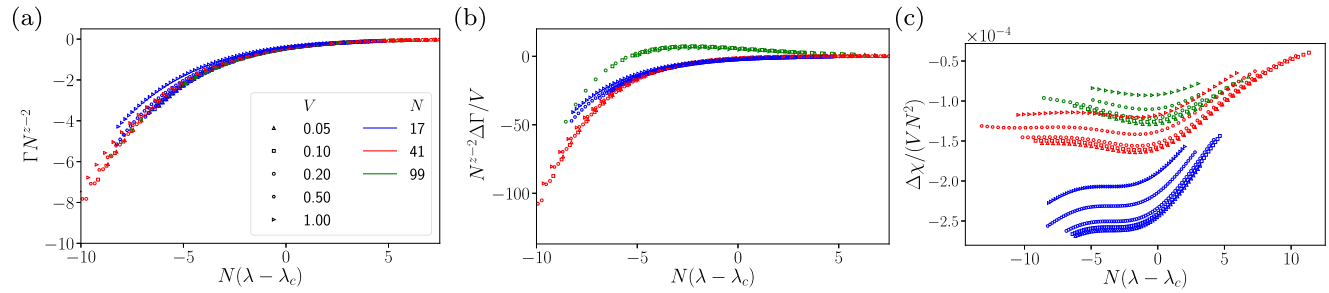

FIG. 5. (a) Even in the presence of interactions, Γ still scales onto the same curve with $\lambda_c \approx 2.0 + 0.23V$, $z = 1.575$, and $\nu = 1$. The legend applies to (a), (b), and (c): each system size N corresponds to a different color, and different symbols correspond to different V. In (b) and (c), it is clear that the change in Γ and χ_F is proportional to V showing that it is likely irrelevant since such proportionality would break down at larger N if it were relevant. There is no collapse onto a single scaling function in (b) and (c) because there are at least two irrelevant directions that V contributes to. Because the collapse is worse for $\Delta\chi$ than for $\Delta\Gamma$, it appears that χ suffers from more finite-size effects.

comparable to one that is achieved by bond dimension m in open boundary conditions, requires m^2 in periodic boundary conditions [70].

The PBC allow us to reliably reach a maximum system size of $\lesssim$200. Since the best rational approximation's denominator N_k grows exponentially, it is difficult to find β which provide enough accessible system sizes. The most dense denominators occur for the golden ratio β_{11}, but due to the three scaling functions at half-filling, there are only two system sizes for each of the three curves with $10 < N_k < 200$, which makes finite-size scaling unreliable. We instead focus on the following three cases: $\beta = 1/\sqrt{2} = \beta_{21}$ at half-filling, $\beta =$ "0" at half-filling, and $\beta = \beta_{11}$ at the commensurate filling $2\beta_{11} - 1$.

For half-filling and $\beta = 1/\sqrt{2}$, all values of N have the same scaling function, and we can easily access three system sizes. In Fig. 5, we notice that χ, Γ still collapse onto the same curves with the same exponents. We determine $\lambda_c \approx 2.0 + \Delta\lambda$ where $\Delta\lambda$ is how much the peak of χ_F shifts for the largest N shown. Since there is no change in the exponent and the curves remain essentially the same, we suspect that V is irrelevant or marginal. We can attempt to estimate the exponent of the irrelevant direction via a finite-size scaling analysis.

We assume the scaling hypothesis of a quantity X to write

$$\begin{aligned} X &= f(|t|N^{1/\nu}, u_1 N^{y_1}, u_2 N^{y_2}, \ldots) \\ &= f(|t|N^{1/\nu}, 0, 0, \ldots) \\ &\quad + \sum_i u_i N^{y_i} f_i(|t|N^{1/\nu}, 0, 0, \ldots), \end{aligned} \tag{19}$$

where t is the parameter tuning the transition, the scaling function is $f(x_0, x_1, x_2, \ldots)$ and $f_i = \partial f/\partial x_i$. Since each u_i is a linear combination of λ, V, and potentially other parameters (if the RG procedure is not closed), then we will not be able to easily collapse the functions onto a universal curve if $u_i \neq 0$ for $i > 1$ or if $|y_2| \gg |y_1|$.

The typical procedure to estimate irrelevant exponents would have us find the constants ν, y_1, and a_1 that provide the best fit $\chi_{F,\max} \sim N^{2/\nu}(1 + a_1 N^{-y_1})$. Due to the small number of accessible system sizes, we instead attempt to see if the curves completely collapse. When we attempt such a collapse in Fig. 5, a single scaling function does not seem to emerge. However, for small V, we are able to obtain a decent collapse of $\Delta\Gamma = \Gamma(V) - \Gamma(0)$ at fixed N onto the same curve as a function of V. This tells us that our results are not suffering from numerical issues as otherwise they would not be proportional to V. We note that the slight nonlinearity in V of $\Delta\chi_F$ is caused by finite-size corrections (as the peak is also shifted by irrelevant parameters). Since the data do not collapse well onto a single curve, we conclude that the interaction term contributes to at least two irrelevant directions. We would therefore need at least four points to fit the $\chi_{F,\max}$ data to estimate the most relevant irrelevant direction, but such an analysis would not be very conclusive. With $\beta = \beta_{nm}$ and incommensurate fillings, there exists no good choice of β that allows for enough accessible system sizes with this current analysis. To access more system sizes, we can consider $\beta =$ "0" by taking $\beta = 1/N$ for any N, as first discussed in Ref. [44]. This parameter choice leads to a very similar transition at half-filling in that, for $V = 0$, $\nu = 1$, $\lambda_c = 2$, and $z = 1.245$ (see Fig. 6 for the free case).[3] To keep the curves within the same universality class at half-filling, we choose N that are divisible by four with $\phi = 0$. Nevertheless, many more system sizes are accessible.[4]

To do the finite-size analysis, we compute $\chi(\lambda_{\max})$ and $\Gamma(\lambda_{\max})$ where $\lambda_{\max}$ is the peak of the fidelity susceptibility (determined with a cubic interpolation of the points at which we performed DMRG). We first observe in Fig. 7 that $\chi_{F,\max} \sim N^{\mu}\log(N)$ with $\mu \approx 2.1$ and $\Gamma(\lambda_{\max}) \sim N^{2-z}(1 + aN^{-y_1})$ with $z \approx 1.2$–1.3, $y_1 \approx 1.1$–1.3 for all cases including the free case. Due to the nicer collapse of Γ in the β_{21} case and to isolate the effect of V, we consider the quantity $[\Gamma(V, \lambda_{\max}) - \Gamma(0, \lambda_{\max})]/\Gamma(0, \lambda_{\max}) \equiv \Delta\Gamma/\Gamma_{\text{free}} \sim N^{-y_V}$ and perform a scaling analysis. Using the scaling hypothesis, we expect this to be the most relevant irrelevant direction that V contributes to. Our analysis gives $0.44 < y_V < 0.48$ when we use system sizes with $N > 60$ for

[3]Reference [44] estimates that the width of the fidelity susceptibility scales with $N^{0.7}$ and the peak scales with $N^{2.25}$. The peak seems to scale with an exponent $\mu > 2$, but we find that with a logarithmic correction taken into account, $\mu \approx 2.1$, instead of $\mu = 2.25$. Additionally, the collapse of Γ strongly suggests $\nu = 1.0$, and, as N gets larger, the fidelity susceptibility curves seem to also collapse better and better onto a curve with width scaling with N.

[4]If we choose $\phi = \pi/2$, the universality classes for all even N are the same, as is predicted by the Diophantine equation.

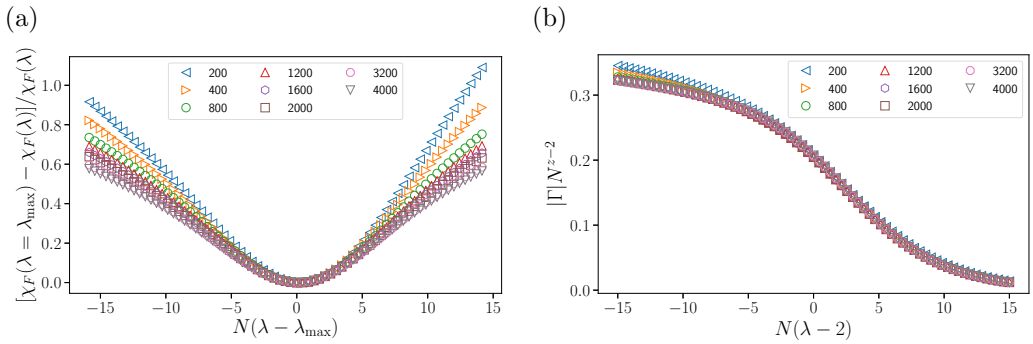

FIG. 6. For $\beta = 1/N$ at filling $N_F = N/2$, we plot the scaling functions χ_F and Γ in (a) and (b), respectively. We extract exponents $\nu = 1.0$, $z = 1.245$, and $\lambda_c = 2.0$. The fidelity susceptibility does not collapse well far from the transition, but Γ does, which is why Ref. [44] underestimated $\nu \approx 0.7$ as the scaling of the width of the curve. When we fit the maximum of $\chi_F \sim L^{\mu} \log(L)$ we find $\mu = 2.1 \approx 2/\nu$ as opposed to the value of $\mu = 2.25$ from Ref. [44] where such a logarithmic correction has not been included.

the fit. When we perform a similar analysis on $\Delta\chi_F/\chi_{F,\text{free}}$, we get $y_V \sim 0$ for low V, but we know from Fig. 5(c) that finite-size effects influence this quantity more. Regardless, the above very much suggests that V is irrelevant or marginal.

Finally, we turn to the commensurate filling of $2\beta_{11} - 1$ for $\beta = \beta_{11}$. Because of the irrelevance of a given interaction V, we expect that at incommensurate filling, the system flows toward the $\lambda = 2, V = 0$ critical point. However, it is unclear if that is true when the transition is at $\lambda = 0$. The authors of Ref. [56] studied a localization-delocalization transition at commensurate filling when $V > \sqrt{2}$ coming from the Peierls-type resonance we discuss above. They were unable to get a scaling collapse in λ, which we focus on.

If it is similar to the incommensurate case, we expect that the transition will shift away from the free point, but the exponent will stay the same. Since $\nu = 2$, the fidelity is less useful as a gauge for the location of the transition as the fidelity does not grow superextensively. We can, however, attempt a finite-size scaling allowing λ_c, z, and ν to vary and minimize the following quantity [60]:

$$\sigma^2 = \frac{1}{2\Delta x} \int_{x_0-\Delta x}^{x_0+\Delta x} dx \langle g(x)^2 \rangle - \langle \tilde{g}(x) \rangle^2,$$
$$g(N^{1/\nu}(\lambda - \lambda_c)) = N^{z-2}\Gamma(\lambda), \tag{20}$$

where we use cubic interpolation of the values of $g(x)$ with no explicit evaluation and where $\langle \cdot \rangle$ is an average over the available N. The results of this fitting are shown in Table III and, for $V = -0.5$ and -1.7, Fig. 8.

In contrast to Ref. [56], the exponents seem to be roughly the same as the ones expected in the free case, namely, $\nu = 2, z = 1$, when we perform the finite-size scaling. It should be noted that there is no clear way to estimate errors on our values because the dominant error would come from the finite-size effects that we are neglecting. Adding in these effects would allow for too many parameters to meaningfully constrain the exponents.

Although the transition is still controlled by the same RG fixed point, there is now a finite range of $\lambda \in (-\lambda_c, \lambda_c)$ where the wave function is extended. Additionally, there are rather large finite-size effects in the fidelity susceptibility at $V = -1.7$, which seem to decrease for $V = -0.5$ (see Fig. 8). This suggests that V is irrelevant or marginal in this case. It is not feasible to perform the same analysis as we did for $\beta =$ "0" because the peak of the fidelity susceptibility is not as reliably close to the transition due to it growing only extensively.

Finally, we note that how the transition depends on V is highly dependent on β. We saw that, at half-filling, $\Delta\lambda \approx 0.23V$ in the case of β_{21} and that $\Delta\lambda \approx V$ for $\beta =$ "0" whereas $\Delta\lambda \approx 0$ for $\beta = \beta_{11}$ [56].

V. CONCLUSIONS

By analyzing the Diophantine equation that naturally arises in the Aubry-André model, we have found that it accurately

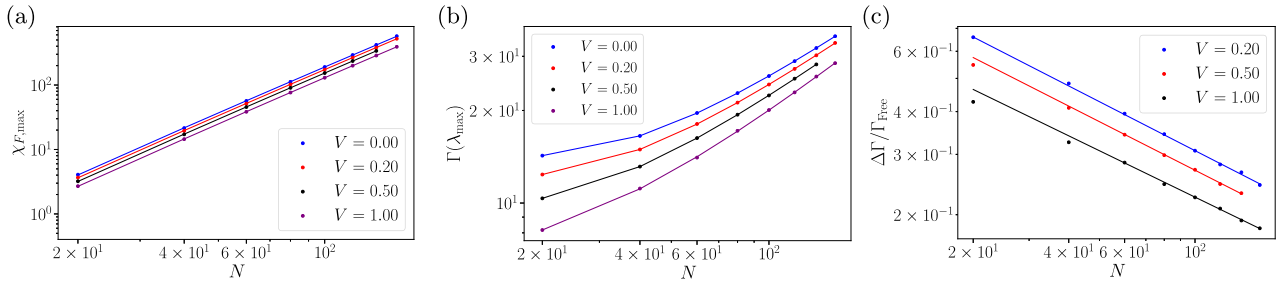

FIG. 7. In (a) we plot the maximum of the fidelity susceptibility occurring at $\lambda = \lambda_{\max}$. The lines indicate a fit to $\chi_{F,\max} \sim N^{\mu} \log(N)$ and $\mu \approx 2.1$ for all interactions. In (b) we plot $\Gamma(\lambda_{\max})$ and fit $\Gamma(\lambda_{\max}) \sim N^{2-z}(1 + a_1 N^{-y_1})$, which all yield $z \approx 1.25$ as in the free case. (c) Depicts $[\Gamma(V, \lambda_{\max}) - \Gamma(0, \lambda_{\max})]/\Gamma(0, \lambda_{\max}) \equiv \Delta\Gamma/\Gamma_{\text{free}} \sim N^{-y_V}$ giving us $y_V \approx 0.44$–0.48 for all V when we exclude points with $N < 60$.

TABLE III. For the first two β's, λ_c is determined from the shift in χ_F for the largest system size probed. In the last case, it comes from finite-size fitting for all $(\lambda_c, 1/\nu, z)$, where all three numbers or a range are reported. Significant figures are chosen to capture the range of values the minimization converges to. The dominant source of error is finite-size effects, which, as mentioned in the text, are difficult to account for or accurately estimate. Since the exponents do not change significantly in any case we considered, we conclude that the Diophantine equation determines the universality class even in the presence of interactions.

β, ρ	V	λ_c
β_{21}, 1/2	0.05	2.011
	0.1	2.023
	0.2	2.046
	0.5	2.119
	1.0	2.249
"0", 1/2	0.2	2.2
	0.5	2.5
	1.0	3.0
β_{11}, $2\beta_{11}-1$	−0.5	(0.05–0.15,0.4,–1)
	−1.3	(0.5, 0.4, –1)
	−1.5	(0.8, 0.4–0.5, –1)
	−1.7	(1.05, 0.51, –0.95)

determines the universality class and, therefore, the dynamic critical exponent $z(\beta, \rho)$ for the incommensurate ratio β and filling factor ρ. This analysis yielded nontrivial relationships between different β and different ρ that show the universality class depends on more than just the continued fraction expansion of β as is seen in the single-particle case [34,40]. The dynamic critical exponent is related to the multifractal properties of the system as it describes how different sections of the energy spectrum scale with system size. The major results testing the Diophantine connection between critical exponents in the noninteracting case are summarized in Table II and explicit examples can be seen in Figs. 2 and 4. The universality class may be measurable either through the low-temperature specific heat (going as $T^{1/z}$) [49], or through the Kibble-Zurek mechanism [50].

Such a relationship may seem contrived or pathological, but we have provided evidence that the exponents are nearly insensitive to the simplest form of interactions (see Table III for β_{11}). Although the exponents do not change, in both the commensurate and incommensurate cases, the location of the transition does change, and that change is dependent on β; in the commensurate case, weak disorder will therefore not guarantee that the wave function will be localized. The degree of irrelevance of the interaction is measured for $\beta =$ "0," but the results are inconclusive. We expect that for large enough interactions, the transition will become first order or cease to exist as large enough V will induce a charge-density wave state [15].

As mentioned, the Diophantine equation arises nonperturbatively due to properties of the magnetic translation group alone in a 2D tight-binding Hamiltonian [58]. We expect that perturbations to Eq. (10) that can be written as perturbations to that 2D tight-binding Hamiltonian should therefore preserve the Diophantine equation description of the universality. This would hold in particular for modified AA models which exhibit a mobility edge in the single-particle spectrum; the only difference being that λ_c would change with the filling factor as states at different energies in the spectrum undergo the

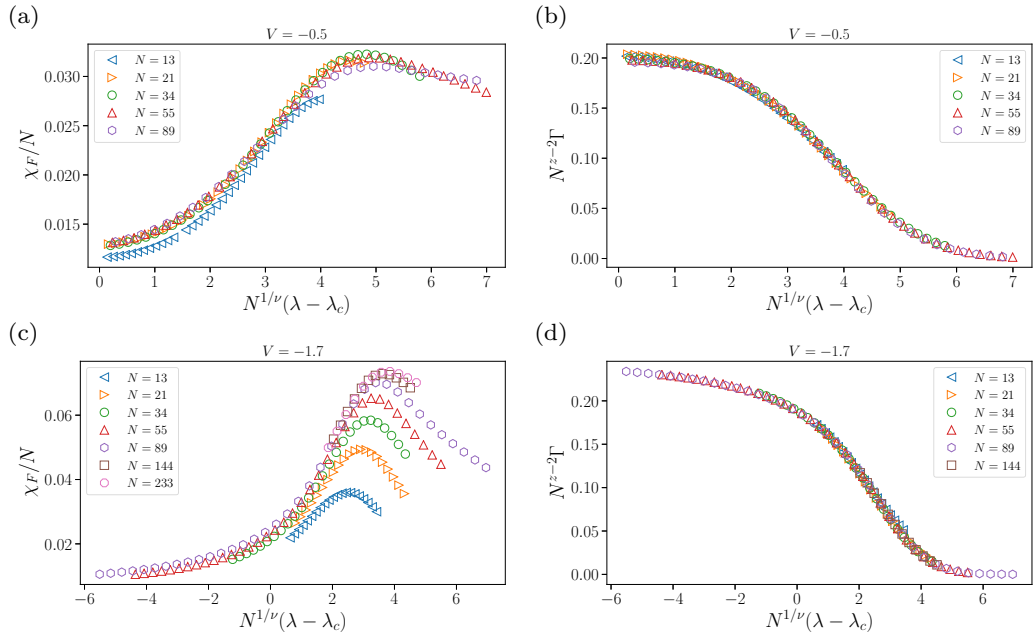

FIG. 8. We plot the scaling collapse of Γ [in (b) and (d)] and χ_F [in (a) and (c)] for commensurate filling $\rho_3 = 2\beta_{11} - 1$ and two different interaction strengths, where the exponents are determined using Γ only. In the free case, $\nu = 2$, $z = 1$, and $\lambda_c = 0$, and the scaling collapse for Γ in (b) and (d) gives $\nu \approx 2.5$, $z \approx 1$, and $\lambda_c \approx 0.05$ for $V = -0.5$ and $\nu \approx 2$ and $z \approx 1$ with $\lambda_c \approx 1$ for $V = -1.7$, so the exponents have not changed much. Although numerically determined, Γ close to the transition should be accurate and less prone to finite-size effects than χ_F. However, finite-size effects are the largest source of error.

localization transition at different values of λ. For instance, the modified Hamiltonian in Ref. [71] with a mobility edge can be derived from a 2D tight-binding Hamiltonian in a magnetic field when there is a second nearest-neighbor hopping in the direction parallel to the gauge field. The generalizations to the AA model introduced in Refs. [36,37] with analytically determined mobility edges, however, do not seem to satisfy the condition of being derived from a 2D Hamiltonian and therefore do not feature the required symmetries. Another possible future direction is the study of transitions in quasi-1D systems with quasiperiodic disorder and mobility edges [72,73].

ACKNOWLEDGMENTS

The authors were supported by NSF Grant No. DMR-1918065 (T.C. and J.E.M.) and by NSF Graduate Research Fellowship Program, NSF Grant No. DGE 1752814 (T.C.), TIMES at Lawrence Berkeley National Laboratory supported by the U. S. Department of Energy, Office of Basic Energy Sciences, Division of Materials Sciences and Engineering, under Contract No. DE-AC02-76SF00515 and by DFG research fellowship No. MO 3278/1-1 (J.M.), and a Simons Investigatorship (J.E.M.).

APPENDIX A: OPERATOR ALGEBRA DERIVATION OF SCALING QUANTITIES

We will derive the numeric expressions we are using. We consider the equation

$$\chi_{F,2+2r} = \sum_{n\neq 0} \frac{|\langle\Psi_n|H_I|\Psi_0\rangle|^2}{(E_n - E_0)^{2+2r}} \sim N^{\mu+2zr} \tag{A1}$$

for the generalized fidelity susceptibility. Since we are considering λ as the tuning parameter, $H_I = \sum_i h_i n_i$. We can switch bases and rewrite

$$H = \sum_{i,j} c_i^\dagger H_{ij} c_j = \sum_i \gamma_i^\dagger \gamma_i \lambda_i \tag{A2}$$

for $\gamma_i = S_{ij} c_j$ since we diagonalize $H_{ij} = S_{ik}^\dagger \Lambda_{kl} S_{lm}$. The ground state with N_F particles will be

$$|\Psi_0\rangle = \gamma_{N_F}^\dagger \gamma_{N_F-1}^\dagger \dots \gamma_1^\dagger |0\rangle, \tag{A3}$$

where the energies λ_i are sorted from least to greatest. In this basis, we can write

$$H_I = \sum_{i,j,k} h_i S_{ji}^\dagger S_{ik} \gamma_j^\dagger \gamma_k \tag{A4}$$

which clearly only drives transitions between the ground state and states $|\Psi_n\rangle$ where we have excited one of the particles to a higher-energy state. Therefore,

$$\chi_{F,2+2r} = \sum_{j>N_F, k\leqslant N_F} \frac{|\sum_i S_{ij}^* S_{ik} h_i|^2}{(\lambda_j - \lambda_k)^{2+2r}}. \tag{A5}$$

There are $N_F(N - N_F)/2$ states that contribute to this sum, so the operator scales as $\mathcal{O}(N^3)$ if $N_F \sim N$. Because diagonalizing the matrix is $\mathcal{O}(N^3)$ anyway, it does not hurt the overall scaling.

To compute $\Gamma = N^2 \partial E/\partial\theta$, we need to do perturbation theory where the perturbation is $H_I = P_F(e^{i\theta} - 1) c_N^\dagger c_1 + P_F(e^{-i\theta} - 1) c_1^\dagger c_N$. We need to compute the coefficient of θ^2. In addition to a term like in $\chi_{F,2+2r}$, there is an additional term from first-order perturbation theory where we have Taylor expanded $e^{i\theta} - 1$ and kept to second order. Therefore,

$$\Gamma = N^2 \left[\sum_i \frac{P_F}{2} (S_{iN}^\dagger S_{1i} + S_{i1}^\dagger S_{Ni}) + \sum_{j>N_F, k\leqslant N_F} \frac{|S_{jN}^\dagger S_{1k} - S_{j1}^\dagger S_{Nk}|^2}{\lambda_j - \lambda_k} \right] \tag{A6}$$

which is $\mathcal{O}(N^2)$.

APPENDIX B: DIOPHANTINE EQUATION MANIPULATIONS

We will derive that (β_{nn}, ρ) and $(\beta_{nn}, \rho/\beta_{nn})$ at incommensurate fillings belong to the same universality class rigorously under our conjecture (i.e., they have the same value of Q_k/N_k for $k \gg 1$). We can use similar manipulations to make the hand-wavy analyses in the main text [such as Eqs. (17) and (18)] more rigorous.

Suppose that we have a solution Q_k, P_k to the Diophantine equation $Q_k M_k - P_k N_k = N_F$. Then, we can use that $M_k/N_k = N_{k-1}/(nN_{k-1} + M_{k-1})$ for β_{nn} to write

$$\begin{aligned} N_F \frac{(nN_{k-1} + M_{k-1})}{N_k} &= Q_k N_{k-1} - P_k (nN_{k-1} + M_{k-1}) \\ &= (Q_k - nP_k) N_{k-1} - P_k M_{k-1}. \end{aligned} \tag{B1}$$

Notice that, in the limit that $k \to \infty$, $N_F = N_k \rho$ and $N_F' = N_F(nN_{k-1} + M_{k-1})/N_k = N_{k-1}\rho/\beta$ where we used $\beta_{nn} = M_k/N_k$. Therefore, the solutions to the Diophantine equation at these two fillings are related. It now suffices to show that $P_k/N_{k-1} = Q_k/N_k$ as $k \to \infty$. Recall that $N_{k-1}/N_k \to \beta_{nn}$ and, as P_k grows extensively for incommensurate fillings, then the Diophantine equation reveals that $M_k/N_k - P_k/Q_k = N_F/(N_k P_k) \to 0$, so $P_k/Q_k \to \beta_{nn}$ as well.

APPENDIX C: DETAILS OF THE DMRG CALCULATIONS

As discussed in the main text, DMRG computations for (A)PBC require larger bond dimension than for open systems. In order to ensure convergence, we use the following procedure. Let $H(\lambda, \theta)$ be the Hamiltonian at the parameter value λ and twist to periodic boundary conditions of θ, and $|\Psi(\lambda, \theta)\rangle$ is the ground-state wave-function candidate achieved by performing DMRG. When $\theta = 0$, we suppress the θ dependence for notational simplicity. For the fidelity, we perform n_1 sweeps on $|\Psi(\lambda)\rangle$ with a maximum bond dimension of M_1. We then start doing two sweeps with a maximum bond dimension at $M_1 + M_2 \lfloor n_{\text{sweeps}}/2 \rfloor$ for n_{sweeps} the total number of sweeps on $|\Psi(\lambda)\rangle$ and $|\Psi(\lambda \pm \delta\lambda)\rangle$ [using $|\Psi(\lambda)\rangle$ as the initial guess]. After the two sweeps, we

TABLE IV. The β's within the same cell belong to the same universality class, based on the analysis of the Diophantine equation alone. The value of p is given, but we omit the sequence of $|Q_k|/N_k$ which differentiates those classes with the same value of p. Note that when β_{pm} has p with a common divisor to $6 = 1/\rho$ the universality classes depend on more than just p, which determines the asymptotic continued fraction expansion of β_{pm}.

Universality class	p
$\beta_{11}, \beta_{12}, \beta_{13}, \beta_{14}, \beta_{15}$	12
$\beta_{21}, \beta_{23}, \beta_{25}, \beta_{27}$	8
$\beta_{22}, \beta_{26}, \beta_{28}$	4
β_{24}	8
$\beta_{31}, \beta_{34}, \beta_{37}$	3
β_{32}, β_{35}	3
β_{33}, β_{36}	6
β_{41}, β_{45}	8
β_{42}, β_{48}	8
β_{43}, β_{47}	8
β_{44}, β_{46}	4

compute

$$\chi_F = -2\frac{\ln\left\{\frac{[\langle\Psi(\lambda)|\Psi(\lambda+\delta\lambda)\rangle+\langle\Psi(\lambda)|\Psi(\lambda-\delta\lambda)\rangle]}{2}\right\}}{\delta\lambda^2} + \mathcal{O}(\delta\lambda^2) \quad \text{(B2)}$$

and compare with the previously computed value. Once the relative change is below ϵ, we consider it converged.

To compute Γ, we follow a similar procedure but we are doing sweeps on $|\Psi(\lambda)\rangle$, $|\Psi(\lambda,\theta_0)\rangle$, $|\Psi(\lambda,2\theta_0)\rangle$, $|\Psi(\lambda,3\theta_0)\rangle$, and we compute Γ as

$$\Gamma = N^2\frac{-245E(0)+270E(\theta_0)-27E(2\theta_0)+2E(3\theta_0)}{90\theta_0^2} + \mathcal{O}(\theta_0^6), \quad \text{(B3)}$$

where $E(\theta)$ is the expectation of the energy of $|\Psi(\lambda,\theta)\rangle$.

We generally use parameters $(n_1, M_1, M_2, \epsilon, \delta\lambda, \theta_0) = (6, 300, 100, 10^{-5}, 0.001, \pi/30)$. We compare the values of χ_F and Γ computed with the above formula as well as those with lower-order finite-difference expressions to ensure reasonable accuracy. We also calculated them in the $V = 0$ case and found good agreement.

APPENDIX D: UNIVERSALITY CLASS AT $\frac{1}{6}$ FILLING

The results presented in this Appendix are solely based on the Diophantine equation. As mentioned in the main text, the two universality classes are considered the same if the same sequence of values of $q_k = |Q_k|/N_k$ appears, and this sequence has a period of p. We omit the sequence of q_k for clarity.

We find the results in Table IV. Notably, the universality classes for β_{1m} for $m \in \{1, 2, 3, 4, 5\}$ are all the same, whereas there are different classes for β_{2m}, β_{3m}, and β_{4m} for a filling of $\rho = \frac{1}{6}$. This evidence supports the notion that β_{pm} can split into different universality classes at a filling of $1/q$ if p and q share a prime divisor, but the details are not obvious. It is not, for instance, that $m \bmod p$ or $m \bmod q$ determines the universality, based on Table IV.

[1] P. W. Anderson, Phys. Rev. **109**, 1492 (1958).
[2] D. Basko, I. Aleiner, and B. Altshuler, Ann. Phys. **321**, 1126 (2006).
[3] I. V. Gornyi, A. D. Mirlin, and D. G. Polyakov, Phys. Rev. Lett. **95**, 206603 (2005).
[4] D. A. Abanin, E. Altman, I. Bloch, and M. Serbyn, Rev. Mod. Phys. **91**, 021001 (2019).
[5] E. van Nieuwenburg, Y. Baum, and G. Refael, Proc. Natl. Acad. Sci. USA **116**, 9269 (2019).
[6] S. Aubry and G. André, Ann. Isr. Phys. Soc **3**, 133 (1980).
[7] P. G. Harper, Proc. Phys. Soc., London, Sect. A **68**, 874 (1955).
[8] D. R. Hofstadter, Phys. Rev. B **14**, 2239 (1976).
[9] M. Kohmoto, Phys. Rev. Lett. **51**, 1198 (1983).
[10] J. Avron and B. Simon, Bull. Am. Math. Soc. (N.S.) **6**, 81 (1982).
[11] V. Mastropietro, Phys. Rev. Lett. **115**, 180401 (2015).
[12] V. Mastropietro, Commun. Math. Phys. **351**, 283 (2017).
[13] S. Iyer, V. Oganesyan, G. Refael, and D. A. Huse, Phys. Rev. B **87**, 134202 (2013).
[14] V. Khemani, D. N. Sheng, and D. A. Huse, Phys. Rev. Lett. **119**, 075702 (2017).
[15] P. Naldesi, E. Ercolessi, and T. Roscilde, Sci. Post. Phys. **1**, 010 (2016).
[16] F. Setiawan, D.-L. Deng, and J. H. Pixley, Phys. Rev. B **96**, 104205 (2017).
[17] S. Bera, T. Martynec, H. Schomerus, F. Heidrich-Meisner, and J. H. Bardarson, Ann. Phys. **529**, 1600356 (2017).
[18] V. P. Michal, B. L. Altshuler, and G. V. Shlyapnikov, Phys. Rev. Lett. **113**, 045304 (2014).
[19] U. Agrawal, S. Gopalakrishnan, and R. Vasseur, Nat. Commun. **11**, 2225 (2020).
[20] M. Žnidarič and M. Ljubotina, Proc. Natl. Acad. Sci. USA **115**, 4595 (2018).
[21] E. V. H. Doggen and A. D. Mirlin, Phys. Rev. B **100**, 104203 (2019).
[22] Y. B. Lev, D. M. Kennes, C. Klöckner, D. R. Reichman, and C. Karrasch, Europhys. Lett. **119**, 37003 (2017).
[23] M. Schreiber, S. S. Hodgman, P. Bordia, H. P. Lüschen, M. H. Fischer, R. Vosk, E. Altman, U. Schneider, and I. Bloch, Science **349**, 842 (2015).
[24] P. Bordia, H. P. Lüschen, S. S. Hodgman, M. Schreiber, I. Bloch, and U. Schneider, Phys. Rev. Lett. **116**, 140401 (2016).
[25] H. P. Lüschen, P. Bordia, S. Scherg, F. Alet, E. Altman, U. Schneider, and I. Bloch, Phys. Rev. Lett. **119**, 260401 (2017).
[26] T. Kohlert, S. Scherg, X. Li, H. P. Lüschen, S. Das Sarma, I. Bloch, and M. Aidelsburger, Phys. Rev. Lett. **122**, 170403 (2019).
[27] G. Roati, C. D'Errico, L. Fallani, M. Fattori, C. Fort, M. Zaccanti, G. Modugno, M. Modugno, and M. Inguscio, Nature (London) **453**, 895 (2008).

[28] Y. Lahini, R. Pugatch, F. Pozzi, M. Sorel, R. Morandotti, N. Davidson, and Y. Silberberg, Phys. Rev. Lett. **103**, 013901 (2009).
[29] A. Purkayastha, S. Sanyal, A. Dhar, and M. Kulkarni, Phys. Rev. B **97**, 174206 (2018).
[30] V. K. Varma, C. de Mulatier, and M. Žnidarič, Phys. Rev. E **96**, 032130 (2017).
[31] S. Saha, S. K. Maiti, and S. Karmakar, Physica E (Amsterdam) **83**, 358 (2016).
[32] A.-K. Wu, S. Gopalakrishnan, and J. H. Pixley, Phys. Rev. B **100**, 165116 (2019).
[33] J. Sutradhar, S. Mukerjee, R. Pandit, and S. Banerjee, Phys. Rev. B **99**, 224204 (2019).
[34] A. Szabó and U. Schneider, Phys. Rev. B **98**, 134201 (2018).
[35] B.-B. Wei, Phys. Rev. A **99**, 042117 (2019).
[36] S. Ganeshan, J. H. Pixley, and S. Das Sarma, Phys. Rev. Lett. **114**, 146601 (2015).
[37] X. Li, S. Ganeshan, J. H. Pixley, and S. Das Sarma, Phys. Rev. Lett. **115**, 186601 (2015).
[38] W. DeGottardi, D. Sen, and S. Vishveshwara, Phys. Rev. Lett. **110**, 146404 (2013).
[39] X. Cai, L.-J. Lang, S. Chen, and Y. Wang, Phys. Rev. Lett. **110**, 176403 (2013).
[40] Y. Hashimoto, K. Niizeki, and Y. Okabe, J. Phys. A: Math. Gen. **25**, 5211 (1992).
[41] I. M. Suslov, Sov. Phys. JETP **56**, 612 (1982).
[42] D. J. Thouless and Q. Niu, J. Phys. A: Math. Gen. **16**, 1911 (1983).
[43] M. Y. Azbel, Phys. Rev. Lett. **43**, 1954 (1979).
[44] M. Thakurathi, D. Sen, and A. Dutta, Phys. Rev. B **86**, 245424 (2012).
[45] S. Ostlund and R. Pandit, Phys. Rev. B **29**, 1394 (1984).
[46] S. N. Evangelou and J.-L. Pichard, Phys. Rev. Lett. **84**, 1643 (2000).
[47] H. Hiramoto and M. Kohmoto, Phys. Rev. B **40**, 8225 (1989).
[48] J. C. C. Cestari, A. Foerster, M. A. Gusmão, and M. Continentino, Phys. Rev. A **84**, 055601 (2011).
[49] C. Tang and M. Kohmoto, Phys. Rev. B **34**, 2041 (1986).
[50] A. Sinha, M. M. Rams, and J. Dziarmaga, Phys. Rev. B **99**, 094203 (2019).
[51] D. J. Thouless, M. Kohmoto, M. P. Nightingale, and M. den Nijs, Phys. Rev. Lett. **49**, 405 (1982).
[52] X. Ni, K. Chen, M. Weiner, D. J. Apigo, C. Prodan, A. Alù, E. Prodan, and A. B. Khanikaev, Commun. Phys. **2**, 55 (2019).
[53] Y. E. Kraus and O. Zilberberg, Phys. Rev. Lett. **109**, 116404 (2012).
[54] Y. E. Kraus, Y. Lahini, Z. Ringel, M. Verbin, and O. Zilberberg, Phys. Rev. Lett. **109**, 106402 (2012).
[55] G. Roux, T. Barthel, I. P. McCulloch, C. Kollath, U. Schollwöck, and T. Giamarchi, Phys. Rev. A **78**, 023628 (2008).
[56] C. Schuster, R. A. Römer, and M. Schreiber, Phys. Rev. B **65**, 115114 (2002).
[57] D.-H. Lee, Philos. Mag. Lett. **73**, 145 (1996).
[58] I. Dana, Y. Avron, and J. Zak, J. Phys. C: Solid State Phys. **18**, L679 (1985).
[59] J. Cardy, *Finite-size Scaling* (Elsevier, Amsterdam, 2012).
[60] M. Newman and G. Barkema, *Monte Carlo Methods in Statistical Physics* (Oxford University Press, New York, 1999).
[61] S.-J. Gu, Int. J. Mod. Phys. B **24**, 4371 (2010).
[62] S. Ray, M. Pandey, A. Ghosh, and S. Sinha, New J. Phys. **18**, 013013 (2015).
[63] J. C. Chaves and I. I. Satija, Phys. Rev. B **55**, 14076 (1997).
[64] M. A. Continentino, Phys. Rev. B **45**, 11312 (1992).
[65] S. Yang, S.-J. Gu, C.-P. Sun, and H.-Q. Lin, Phys. Rev. A **78**, 012304 (2008).
[66] C. De Grandi, V. Gritsev, and A. Polkovnikov, Phys. Rev. B **81**, 012303 (2010).
[67] V. Mastropietro, Phys. Rev. B **93**, 245154 (2016).
[68] S. R. White, Phys. Rev. Lett. **69**, 2863 (1992).
[69] ITensor Library (version 2.1.1) http://itensor.org
[70] U. Schollwöck, Ann. Phys. **326**, 96 (2011).
[71] C. M. Soukoulis and E. N. Economou, Phys. Rev. Lett. **48**, 1043 (1982).
[72] J. D. Bodyfelt, D. Leykam, C. Danieli, X. Yu, and S. Flach, Phys. Rev. Lett. **113**, 236403 (2014).
[73] C. Danieli, J. D. Bodyfelt, and S. Flach, Phys. Rev. B **91**, 235134 (2015).